



THE APPLICATION OF GEOELECTRIC SURVEY TECHNIQUE TO EVALUATE AQUIFER POTENTIALS AND ITS PROTECTIVE CAPACITY IN PARTS OF THREE ARMS ZONE, MINNA, NORTH-CENTRAL NIGERIA

¹Alhassan, A. A., ¹Alhassan, D. U., *¹Shehu, J., ¹Alkali, A. and ²Mohammed, A.

¹Department of Physics, Federal University of Technology, Minna

²Department of Physics, Niger State College of Education, Minna

*Corresponding Author's Email: jameeelshehu@futminna.edu.ng

ABSTRACT

Geoelectric survey was carried out in part of Three Arms Zone Minna, north central Nigeria. The aim of the survey is to evaluate the aquifer potential of the area and its protective capacity. Forty eight vertical electrical sounding stations were investigated across the area. Schlumberger electrode configuration with maximum current electrode spacing (AB/2) of 100 m was employed. The area was gridded into six profiles with profile separations of 100 m and VES spacing of 100 m apart. Two to four geologic layers were delineated from the interpreted results. The geoelectric layers of the subsurface shows topsoil with resistivity range from 2.1 to 434.4 Ωm . Weathered/fractured basement layer resistivity range from 20.4 to 4491.1 Ωm and Fresh basement resistivity ranging between 1,021.4 and 19,418.4 Ωm . The weathered/fractured layer is considered as the major aquiferous zone. Iso-resistivity and longitudinal conductance maps were produced. Eight VES points were consider as the aquifer potential of the area having weathered/fractured resistivity varying between 108.5 Ωm and 647.1 Ωm with thickness range from 11.8 m to 30.7 m. The longitudinal conductance value ranges from 0.002642 Siemens to 2.340909 Siemens. The protective capacity evaluated shows that about 50% of VES points are poorly protected, 14.48% are weakly protected, 22.92% are moderately protected and 12.50% have good protective capacity.

Keywords: Geoelectric Survey, Protective Capacity, Aquifer Potential and Longitudinal Conductance.

INTRODUCTION

The development of any area is a function of availability of basic amenities like water, roads, electricity and industries among others. The growing demand for portable water supply has been the major problem of most urban centres in Nigeria (Alhassan *et al.*, 2015). To meet the water needs of the ever growing population and urbanisation of Minna, groundwater is in high demand. The knowledge of aquifer potential and its protective capacity is essential for sustainable development of the area. This is because good aquifer protective capacity prevent infiltration of leachate into the groundwater.

The area is located at the central part of Nigeria with latitudes 9°28'N to 9°37'N and longitudes 6°23'E to 6°29'E. Geophysical investigation applies the principle of physics to the study of the earth (usually the earth's surface). In other to achieve this, measurements are made at or near the earth surface to obtain data, the interpretation of this data obtained are capable of dictating and delineating local and regional features that could be of economic interest which are uncommon in nature such as anomalies.

The exploration and exploitation of groundwater as a major resource to meet the growing population in urban cities in Nigeria located on basement complex have been the concern of scientist. Availability of groundwater in unconfined aquifers

underlain by impermeable crystalline igneous and/or metamorphic rocks is often controlled by the development of secondary porosity and permeability from weathering and fracturing (Kearey *et al.*, 2002).

The use of geophysical methods for both groundwater resource mapping and water quality evaluation has increased dramatically over the last decade due to rapid advances in electronic technology and the development of numerical modeling solutions. Although various hydro-geophysical techniques are available, electrical resistivity is a popular method because of its low cost, simple operation and efficiency in areas with high contrasting resistivity.

Among several geophysical methods employed to determine depth to bedrock (electrical resistivity, gravity, seismic, magnetic, remote sensing, and electromagnetic), the electrical resistivity method is the most effective (Kearey *et al.*, 2002). It is an effective and a reliable tool in slicing the earth into geoelectric layers. It has the advantage of non-destructive effect on the environment, cost effective, rapid and quick survey time and less ambiguity in interpretations of results when compared to other geophysical survey methods. The vertical electrical sounding (VES) technique provides information on the vertical variations in the resistivity of the ground with depth (Alhassan *et al.*, 2017). It is used to solve a wide variety of problems, such

as; determination of depth, thickness and boundary of aquifer (Daniel *et al.*, 2016). Basement complex is made up of metamorphic and crystalline rocks formed due to volcanic activities (such rocks like gneiss, schist, slates, quartzite and phyllites). In Basement Complex, volcanic rocks are formed as a result of eruption of molten magma. As they cool rapidly, fractures are produced and these fractures allow significant water movement. Metamorphic and crystalline rocks are impermeable to water movement. However, fractures that occur in these rocks can allow water movement (McGinley, 1969).

Geology of the Area

Minna occupies the central portion of the Nigeria basement complex. The Minna area comprises of meta-sedimentary and meta-igneous rocks which have undergone polyphase deformation and metamorphism. These rocks have been intruded by granitic rocks of Pan-African age (Ajibade, 1980).

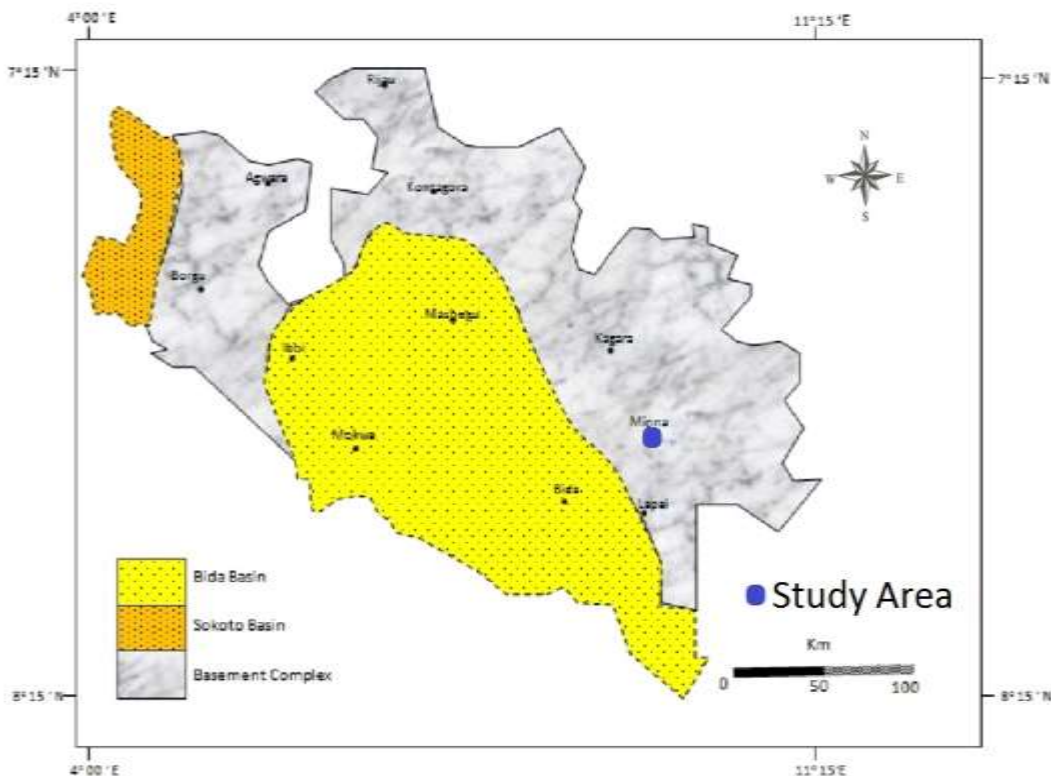


Fig. 1: Geological map of Niger state basement complex and sedimentary basin.

Five lithostratigraphic units have been recognized in Minna area. The schist which occur as a flat laying narrow southwest – northeast belt at the central part of Minna with small quartzite ridge parallel to it, the gneiss occur as a small suites at the northern and southern part of the area forming a contact with the granite (Ajibade, 1980). Feld spathic rich pegmatite is bounded to east, with average width of 65 metres and 100 metres long, the pegmatite hosts tourmaline. Granitic rocks dominate the rock types in the area and vary in texture and composition. The area mapped is underlain by rock of granitic origin and schist intrusion which can be grouped into two on the basis of texture. The rock types are believed to be part of the older granite suite and are mostly exposed along the drainage channel, where they appear in most cases weathered.

Methodology

The area was gridded into six profiles and each profile is 700 metres long. The VES spacing and profile spacing is 100 m apart. The Schlumberger electrode configuration was used. Forty eight VES points were covered, direct current was introduced into the ground and the resulting potential difference measured across two other electrodes. The ratio of the potential difference to the current is displayed by the Terrameter as resistance, as the electrode spacing is progressively increased. The apparent resistivity was computed using equation 1.

$$\rho_a = KR \quad (1)$$

where
 ρ_a is an apparent resistivity

$R = \frac{\Delta V}{I}$, is the earth resistance (2)

$K = \pi \left[\frac{(AB/2)^2 - (MN/2)^2}{MN} \right]$ is the geometric factor (3)

The apparent resistivity values obtained from equation (1) were plotted against the half current electrode separation spacing using WinResist software. From the plots, Vertical electrical sounding curves were obtained (Figure 2). Qualitative deductions such as resistivity of the layers, the depth of each layer, the thickness of each layer, number of layers and curve types were generated.

The Dar-Zarouk parameter of longitudinal conductance (S) of the aquifer layer was used as the basis of aquifer protective capacity. The protective capacity is assessed using the longitudinal conductance which determines the capacity to prevent leachate infiltration into the groundwater repository. It indicates the ability of the characteristics of the subsurface to

prevent or favour leachate percolation. For horizontal, homogenous and isotropic layer, the Dar-Zarouk parameters of longitudinal conductance (S) is given as:

$$S = \sum_{i=0}^n \frac{h_i}{\rho_i} \text{ (Siemens)} \quad (4)$$

where ρ_i and h_i are the resistivity and thickness of the i^{th} layer respectively.

RESULTS AND DISCUSSION

The VES curve produced from apparent resistivity plot against current electrode spacing (AB/2) is presented as Figure 2. From the figure, layer resistivities, depth of the layer, layer thickness and curve types were deduced and used in conjunction with geology and borehole information of the area to delineate the aquifer potentials of the area.

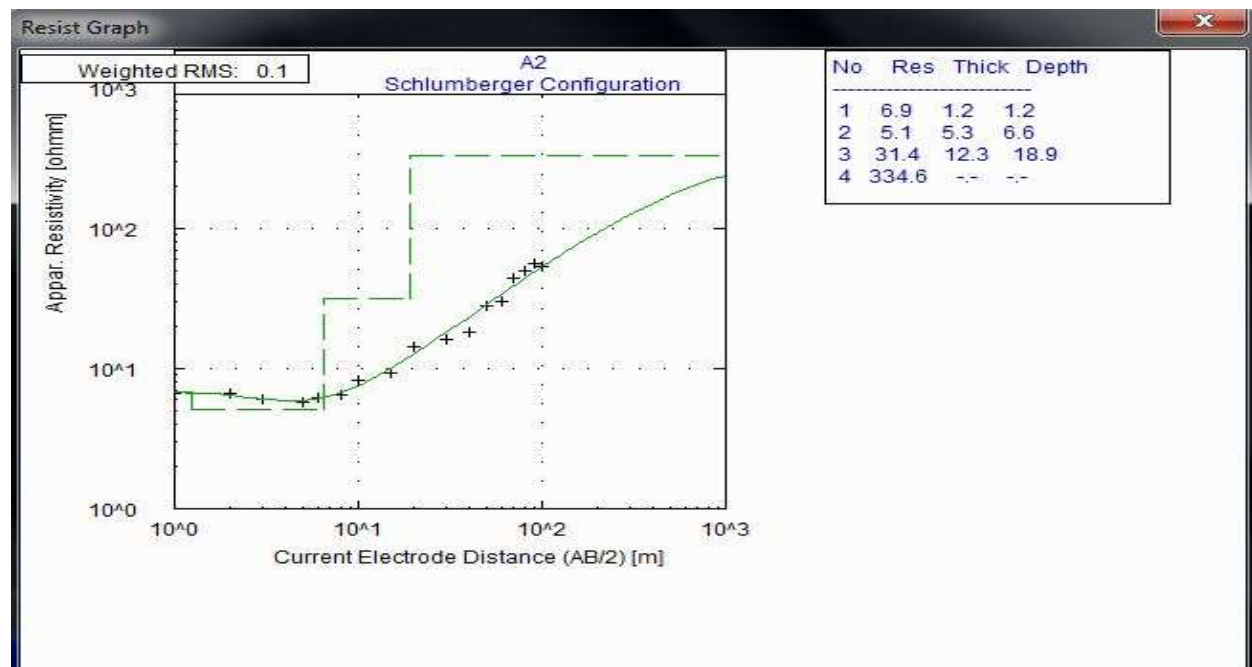


Fig. 2: Vertical Electrical Sounding Curve.

The summary of the resistivity results is presented in Tables 1 to 6. The profile A revealed two to three layers. It is characterised with three distinct curve types which are A, H and KH types. The first layer has resistivity values ranging from 6.1 Ωm to 395.3 Ωm . The lowest resistivity value of 6.1 Ωm found at VES A₅ with the highest resistivity value of 395.3 Ωm found at A₃. The layer was thickest at about 19.4 m at VES A₆ and thinnest at about 0.4 m at VES A₇. The layer was deepest at about 19.4 m at VES A₆ and shallowest at about 0.4 m at VES A₇. The second layer has resistivity values between 104.1 Ωm to 1,401.2

Ωm . The highest resistivity value of this layer is 1,401.2 Ωm found at VES A₈, while the lowest resistivity value is about 104.1 Ωm found at VES A₄. The layer was thickest at about 60.8 m at VES A₃ and thinnest at about 1.9 m at VES A₇. The layer was deepest at about 62.1 m at VES A₃ and shallowest at about 2.3 m at VES A₇. The third layer has resistivity values ranging between 1021.4 Ωm to 19,418.4 Ωm . The highest resistivity value of 19,418.4 Ωm is found at VES A₈, while the lowest resistivity value of 1021.4 Ωm is located at VES A₃.

Table 1: Summary of VES analysis along profile A

VES Points	Curve type	Layer Number	Depth (m)	Thickness (m)	Resistivity (Ωm)
A ₁	H	1	0.0	12.4	15.65
		2	12.4	-	151.4
A ₂	A	1	0.0	18.9	18.7
		2	18.9	-	334.6
A ₃	KH	1	0.0	1.3	395.3
		2	1.3	60.8	615.55
		3	62.1	∞	1021.4
A ₄	A	1	0.0	1.0	17.1
		2	1.0	25.4	104.1
		3	26.4	∞	1811.0
A ₅	A	1	0.0	1.0	6.1
		2	1.0	-	152.45
A ₆	K	1	0.0	19.4	53.15
		2	19.4	-	129.3
A ₇	A	1	0.0	0.4	27.6
		2	0.4	1.9	692.9
		3	2.3	∞	1,371.1
A ₈	A	1	0.0	4.1	51.1
		2	4.1	4.6	1,401.2
		3	8.7	∞	19,418.4

The summary of the resistivity results for profile B is shown in Table 2. This profile shows two to four layer models with two distinct curve types which include A and K curve types. The first layer has a resistivity value ranging from 7.7 Ωm to 232.05 Ωm . The highest resistivity value of the layer is 232.05 Ωm found at VES B₈, while the lowest resistivity of 7.7 Ωm located at VES B₄. The layer's highest thickness of about 25.8 m at VES B₈ and the lowest thickness of about 0.9 m located at B₅. The layer was deepest at about 25.8 m at VES B₈ and shallowest at about 0.9 m located at B₅. The second layer has resistivity values ranging from 37.65 Ωm to 748.6 Ωm . The highest resistivity value of the layer is 748.6 Ωm found at VES B₈, while the lowest resistivity value 37.65 Ωm is found at VES B₂. The layer is thickest at VES B₃ is about 18.2 m and thinnest at VES B₅ is 1.10m. The layer was deepest at about 23.4 m at VES B₃ and shallowest at about 2.0m at VES B₅. The third layer has resistivity values ranging between 1261.1 Ωm to 5101.35 Ωm . The highest resistivity value of 5101.35 Ωm found at VES B₁ and the lowest resistivity value of 1261.1 Ωm located at VES B₃. The fourth layer has resistivity value of 10,871 Ωm .

The summary of the resistivity results for profile C is presented in Table 3. The profile reveal two to three layer models with two distinct curve types A and K. The first layer has a resistivity value ranging from 4.0 Ωm to 312.4 Ωm . The highest resistivity value of the layer is 312.4 Ωm found at VES C₇, while the lowest resistivity of 4.0 Ωm located at VES C₅. The layer's highest thickness of 19.1 m at VES C₂ and the lowest thickness of 0.4 m located at C₅. The layer was deepest at about 19.1 m at VES C₂ and shallowest at about 0.4 m at VES C₅. The second layer has resistivity values ranging from 45.6 Ωm to 4,491.1 Ωm . The highest resistivity value of the layer is 4,491.1 Ωm found at VES C₈, while the lowest resistivity value of 45.6 Ωm is found at VES C₂. The layer is thickest at VES C₈ is about 55.9 m and thinnest at VES C₅ is about 2.6 m. The layer was deepest at about 58.6 m at VES C₈ and shallowest at about 3.1m at VES C₅. The third layer has resistivity values ranging between 1,079.2 Ωm to 7909.4 Ωm . The highest resistivity value of 7909.4 Ωm found at VES C₅ and the lowest resistivity value of 1079.2 Ωm located at VES C₆.

Table 2: Summary of VES analysis along profile B

VES Points	Curve type	Layer Number	Depth (m)	Thickness (m)	Resistivity (Ωm)
B ₁	K	1	0.0	2.2	11.3
		2	2.2	1.5	90.0
		3	3.7	∞	5101.35
B ₂	A	1	0.0	3.1	9.9
		2	3.1	-	37.65
B ₃	A	1	0.0	5.2	174.8
		2	5.2	18.2	413.3
		3	23.4	∞	1261.1
B ₄	A	1	0.0	1.8	7.70
		2	1.8	10.3	87.8
		3	12.1	∞	1743.1
B ₅	A	1	0.0	0.9	9.6
		2	0.9	1.1	218.8
		3	2.0	11.9	3913.5
		4	13.9	∞	10,789.1
B ₆	A	1	0.0	1.2	213.7
		2	1.2	11.7	365.6
		3	12.9	∞	2744.9
B ₇	A	1	0.0	3.1	20.4
		2	3.1	17.6	437.8
		3	20.6	∞	1796.6
B ₈	A	1	0.0	25.8	232.05
		2	25.8	-	748.6

Table 3: Summary of VES analysis along profile C

VES Points	Curve type	Layer Number	Depth (m)	Thickness (m)	Resistivity (Ωm)
C ₁	A	1	0.0	11.1	7.0
		2	11.1	-	45.65
C ₂	A	1	0.0	19.1	13.2
		2	19.1	-	45.6
C ₃	A	1	0.0	18.9	41.15
		2	18.9	-	126.0
C ₄	A	1	0.0	8.1	113.3
		2	8.1	15.2	1119.2
		3	23.3	∞	6,310.7
C ₅	K	1	0.0	0.4	4.0
		2	0.4	2.6	990.8
		3	3.1	∞	7909.4
C ₆	A	1	0.0	5.6	57.8
		2	5.6	23.7	309.2
		3	29.3	∞	1079.2
C ₇	A	1	0.0	2.7	312.4
		2	2.7	17.2	566.0
		3	19.9	∞	2325.5
C ₈	K	1	0.0	2.7	44.4
		2	2.7	55.9	4491.1
		3	58.6	∞	2242.8

The results of profile D is summarised in table 4. The profile shows two to three layer models with only curve type A. The first layer has a resistivity value ranging from 2.1 Ωm to 434.4 Ωm . The highest resistivity value of the layer is 434.4 Ωm found at VES D₆, while the lowest resistivity of 2.1 Ωm found at VES D₅. The layer's highest thickness of about 9.7 m at VES D₃ and the lowest thickness of about 3.0 m located at VES D₅ and D₈. The layer was deepest at about 9.7 m at VES D₃ and shallowest at about 3.0m at VES D₅ and D₈. The second layer has resistivity values ranging from 49.5 Ωm to 756.9 Ωm . The highest resistivity value of the layer is 756.9 Ωm found at VES D₃, while the lowest resistivity value 49.5 Ωm is found at VES D₁. The layer is thickest at VES D₆ is about 30.7 m and thinnest at VES D₃ is about 8.9 m. The layer was deepest at about 36.0 m at VES

D₈ and shallowest at about 14.8 m at VES D₂. The third layer has resistivity values ranging between 1,159.4 Ωm and 7,111.9 Ωm . The highest resistivity value of 7,111.9 Ωm found at VES D₃ and the lowest resistivity value of 1,159.4 Ωm observed at VES D₆.

The result of profile E was summarised in table 5. Two to three layer models were observed having curve types A and K. The first layer has resistivity value ranging from 11.4 Ωm to 102.7 Ωm . The highest resistivity value of 102.7 Ωm found at VES E₄ and the lowest resistivity of 11.4 Ωm located at VES E₁. The thickest layer at VES E₂ is about 41.4 m and the thinnest layer at E₈ is about 1.4 m. The layer was deepest at about 8.5 m located at VES E₃ and E₅ with the shallowest at about 1.4 m

located at VES E₈. The second layer has resistivity value ranging from 102.0 Ωm to 449.95 Ωm. The highest resistivity of 449.95 Ωm found at VES E₃ and the lowest resistivity value of 102.0 Ωm found at VES E₂. The thickest layer at VES E₁ is about 14.5 m and the thinnest layer at VES E₈ is about 10.1m. The layer

was deepest at about 17.8 m located at E₁ with the shallowest at about 11.5 m located at VES E₈. The third layer has resistivity value ranging from 1,165.8 Ωm to 10,412.0 Ωm. The highest resistivity of 10,412.0 Ωm found at VES E₈ and the lowest resistivity value of 1,165.8 Ωm found at VES E₁.

Table 4: Summary of VES analysis along profile D

VES Points	Curve type	Layer Number	Depth (m)	Thickness (m)	Resistivity (Ωm)
D ₁	A	1	0.0	6.8	5.4
		2	6.8	-	49.5
D ₂	A	1	0.0	9.6	26.85
		2	9.6	-	471
D ₃	A	1	0.0	9.7	104.7
		2	9.7	8.9	756.9
		3	18.6	∞	7,111.9
D ₄	A	1	0.0	5.8	7.4
		2	5.8	-	59.3
D ₅	A	1	0.0	3.0	2.1
		2	3.0	-	133.15
D ₆	A	1	0.0	5.3	434.4
		2	5.3	30.7	647.1
		3	36.0	∞	1159.4
D ₇	A	1	0.0	3.2	68.3
		2	3.2	12.2	614.7
		3	15.5	∞	3412.5
D ₈	A	1	0.0	3.0	25.6
		2	3.0	11.8	317.7
		3	14.8	∞	1724.4

Table 5: Summary of VES analysis along profile E

VES Points	Curve type	Layer Number	Depth (m)	Thickness (m)	Resistivity (Ωm)
E ₁	A	1	0.0	3.3	11.40
		2	3.3	14.5	108.5
		3	17.8	∞	1165.8
E ₂	A	1	0.0	41.4	34.35
		2	41.4	-	102.0
E ₃	A	1	0.0	8.5	11.8
		2	8.5	-	449.95
E ₄	K	1	0.0	4.1	102.7
		2	4.1	-	311.95
E ₅	A	1	0.0	8.5	42.1
		2	8.5	-	392.55
E ₆	A	1	0.0	19.2	46.25
		2	19.2	-	261.9
E ₇	A	1	0.0	4.2	101.7
		2	4.2	11.9	396.0
		3	16.1	∞	6771.6
E ₈	A	1	0.0	1.4	100.3
		2	1.4	10.1	106.3
		3	11.5	∞	10,412.0

The summary of the results of profile F is shown in Table 6. The profile shows two to three layer models with curve types A, K and HK. The first layer has resistivity values ranging from 3.4 Ωm to 124.85 Ωm . The highest resistivity value of 124.85 Ωm is located at VES F₄ and lowest resistivity value of 3.4 Ωm is found at VES F₇. The thickest of the layer is about 13.1 m located at VES F₄ and the thinnest of this layer is about 0.4m located at VES F₇ and F₈. The layer was deepest at about 13.1

m located at VES F₄ with the shallowest at about 0.4 m located at VES F₇ and F₈. The second layer has resistivity value ranging from 20.4 Ωm to 946 Ωm . The highest resistivity value of 946 Ωm is located at VES F₄ and lowest resistivity value of 20.4 Ωm is found at VES F₁. The thickness of the layer is about 22.1 m located at VES F₈. The layer has a depth of about 22.5 m located at VES F₈. The third layer has highest resistivity value of 1,111.6 Ωm , found at VES F₈.

Table 6: Summary of VES analysis along profile F

VES Points	Curve type	Layer Number	Depth (m)	Thickness (m)	Resistivity (Ωm)
F ₁	A	1	0.0	7.8	5.8
		2	7.8	-	20.4
F ₂	A	1	0.0	3.1	93.3
		2	3.1	-	346.05
F ₃	A	1	0.0	8.0	39.8
		2	8.0	-	220.35
F ₄	A	1	0.0	13.1	124.85
		2	13.1	-	946.0
F ₅	HK	1	0.0	12.0	18.65
		2	12.0	-	319.65
F ₆	A	1	0.0	8.2	67.5
		2	8.2	-	126.7
F ₇	K	1	0.0	0.4	3.4
		2	0.4	-	779.85
F ₈	A	1	0.0	0.4	6.3
		2	0.4	22.1	35.1
		3	22.5	∞	1111.6

Iso-Resistivity Maps

Figure 3 shows the iso-resistivity map at the surface. The map was drawn at contour interval of 50 Ωm . The map shows spatial variation of the resistivity of the topmost surface features like exposed outcrops. The entire surface of the study area show very low resistivity ranging between 0.7 Ωm to 436.67 Ωm which cover most part the area. Based on the resistivity values, the rock types at the surface may be alluvium and sand topsoil.

The iso-resistivity contour map at 5 m depth was contoured at 50 Ωm interval as shown in Figure 4. The resistivity value of 5.75 Ωm to 584.45 Ωm was observed in all area. The resistivity value of 580 Ωm was found prominent at the north-western part of the area. They are weathered basement rocks.

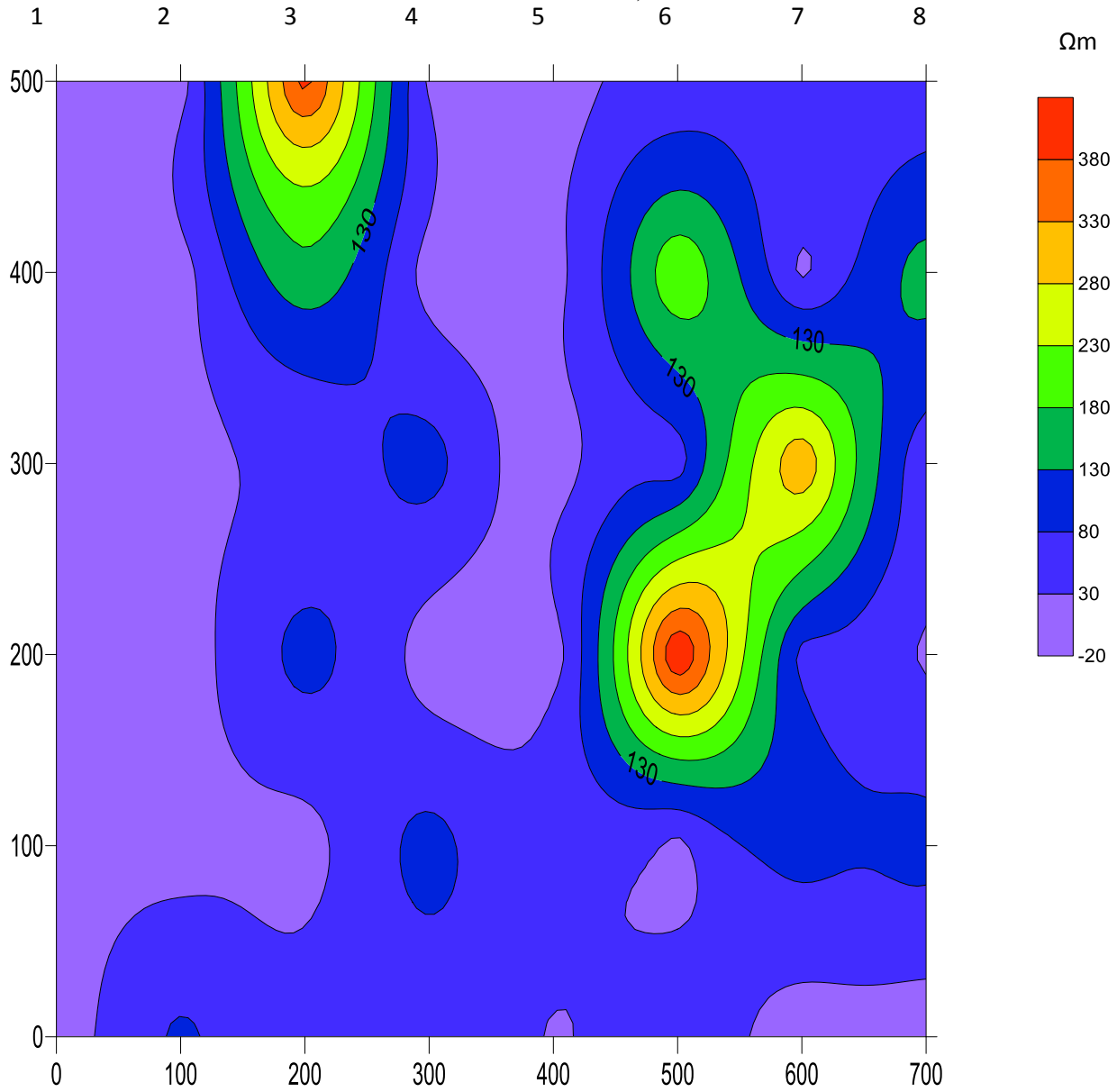


Fig. 3: Iso-resistivity Contour Map at The Surface

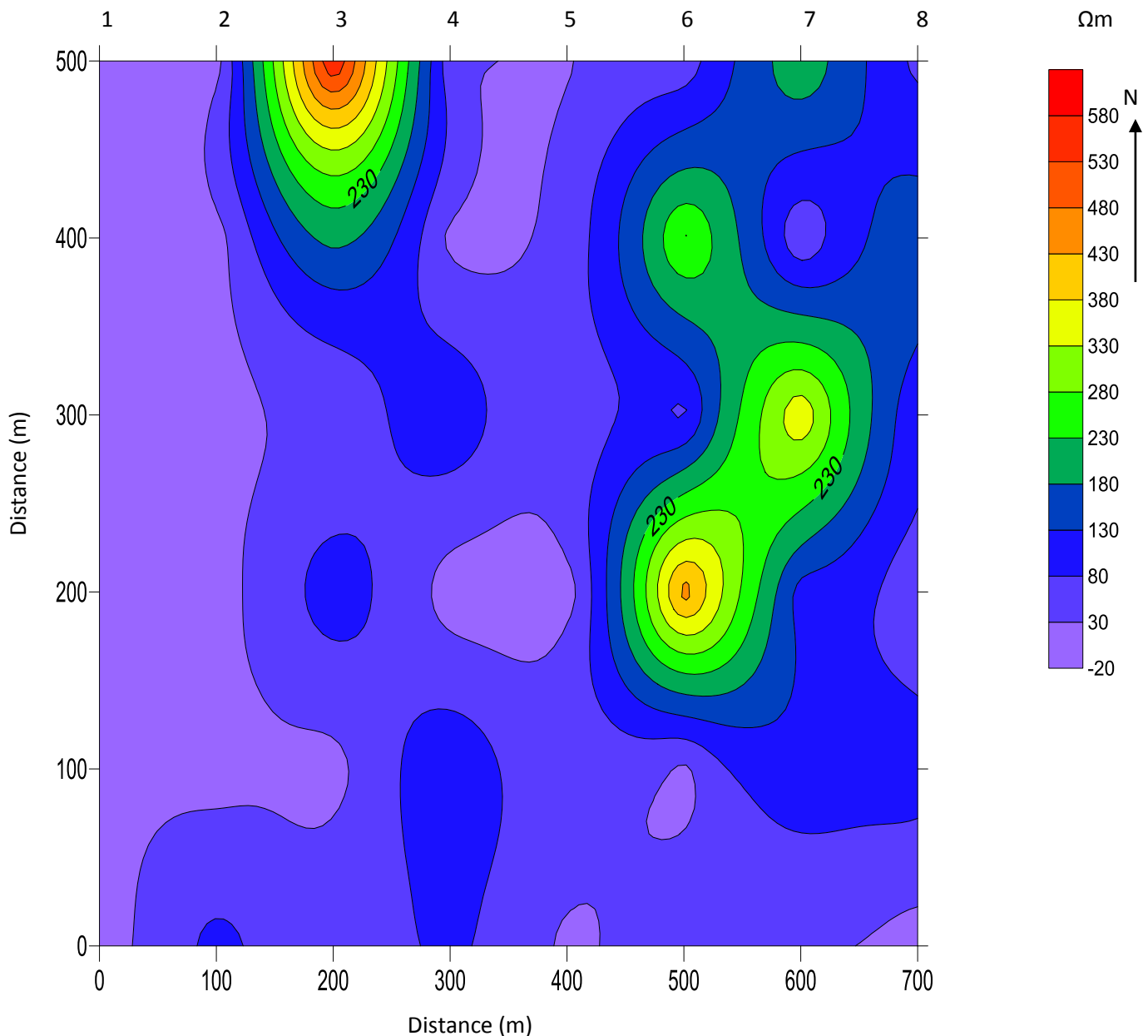


Fig. 4: Iso-resistivity Contour Map at Depth 5 m

The iso-resistivity contour map at 10 m depth was contoured at 50 Ωm interval as shown in Figure 5. The resistivity value of 5 Ωm to 200 Ωm was observed in the central, south western and southern part show nearly saturated horizons. The north-western, north-eastern and south-eastern parts of the area are prominent with resistivity value ranging between 250 Ωm and 700 Ωm which indicates fractured or fairly weathered basement.

The iso-resistivity contour map at 15 m depth was contoured at 50 Ωm interval as shown in figure 6. This differs from depth 10 m such that the resistivity increases slowly north-eastwards and south-eastwards of the map. The resistivity value of about 10 Ωm to 750 Ωm could be observed in all area. The resistivity

value of 10 Ωm to 200 Ωm was observed in the central, south-western and southern part may likely show saturated and nearly saturated horizons. The north-western, north-eastern and south-eastern parts of the area are prominent with resistivity value ranging between 250 Ωm and 750 Ωm which indicates fractured or fairly weathered basement.

The iso-resistivity contour map at 20 m depth was contoured at 50 Ωm interval as shown in figure 7. It is similar to 15 m depth. The resistivity value of 10 Ωm to 200 Ωm was observed in some parts of the map and likely shows saturated and nearly saturated horizons. The resistivity range at this depth is 10 Ωm to 750 Ωm which indicates weathered and fractured basement rock.

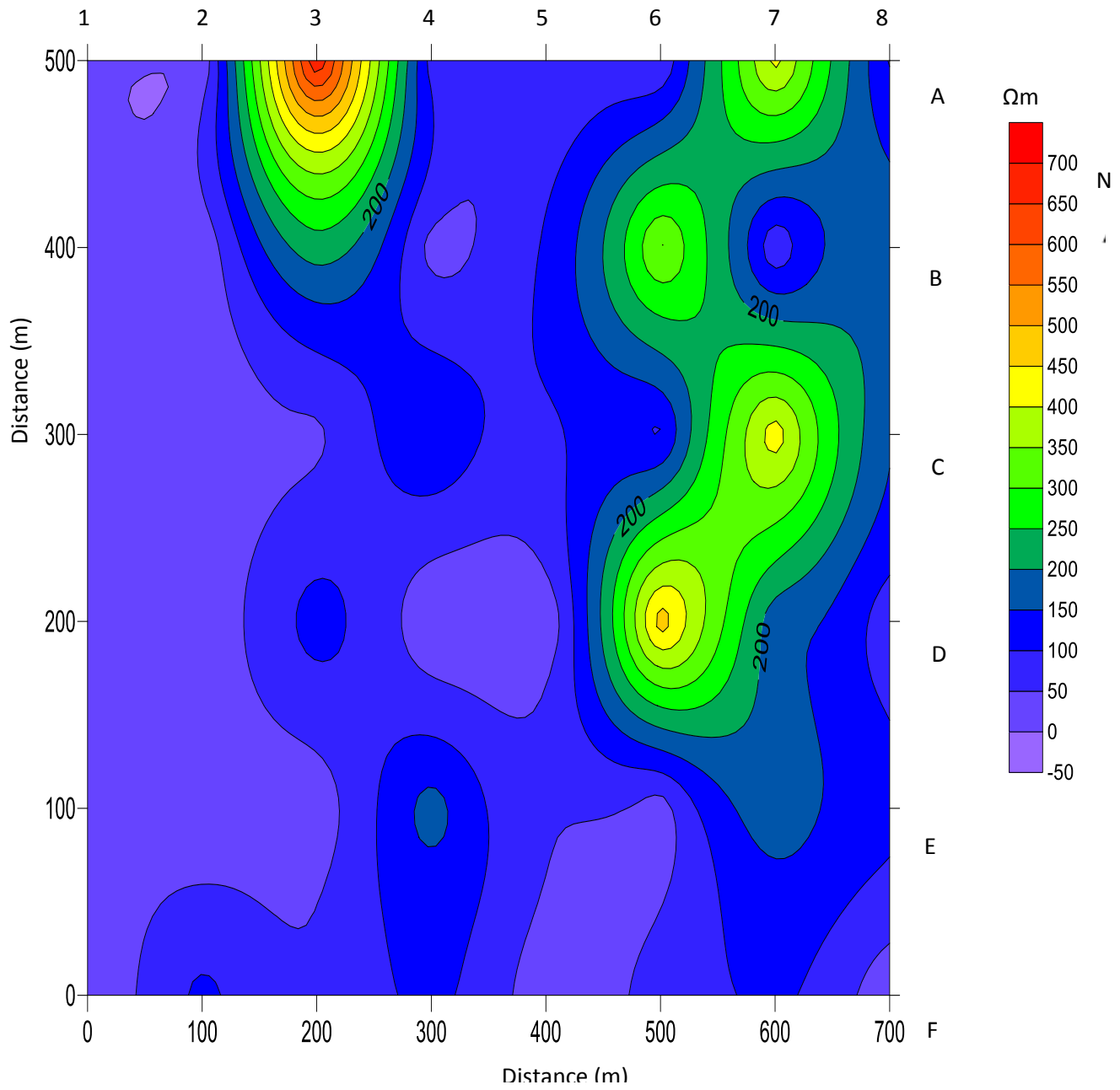


Fig. 5: Iso-resistivity Contour Map at the depth 10 m

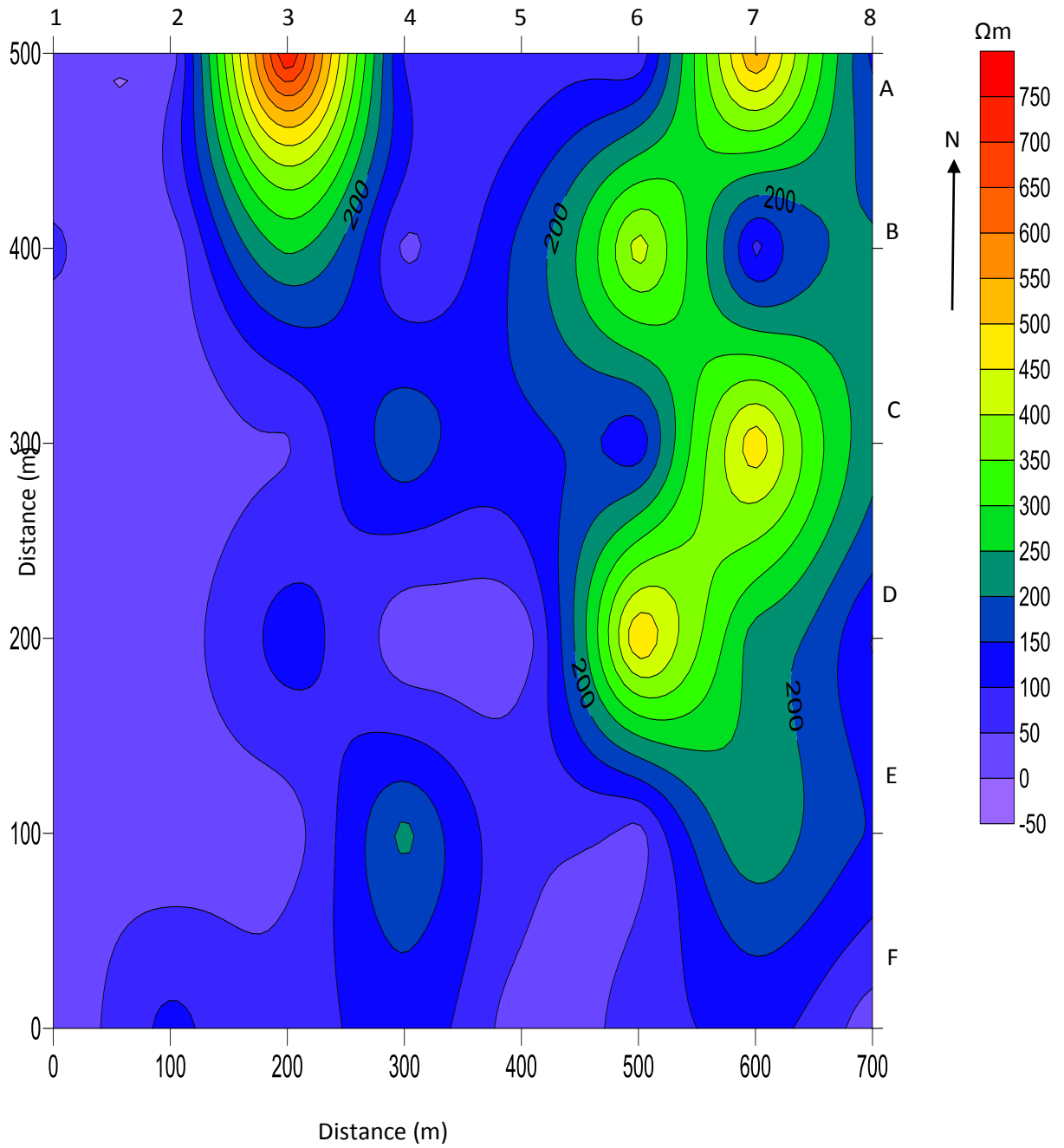


Fig. 6: Iso-resistivity Contour Map at the depth 15 m

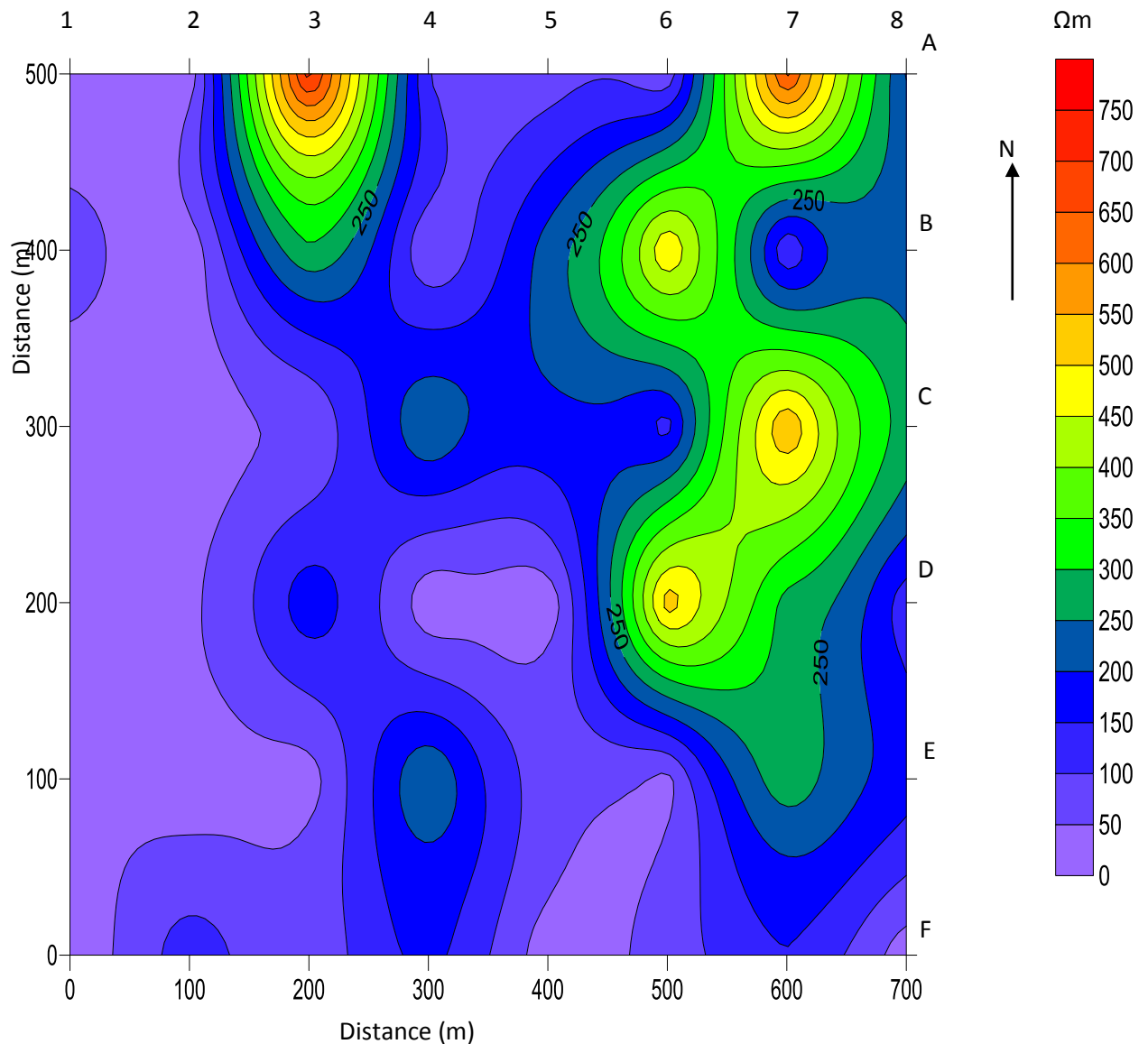


Fig. 7: Iso-resistivity Contour Map at the depth 20 m

The Iso-resistivity contour map at 25 m depth was contoured at 50 Ωm interval as shown in Figure 8. The resistivity range at this depth is 9.88 Ωm to 733.82 Ωm which indicates weathered and fractured basement rock. The resistivity value of 10 Ωm to 200 Ωm was observed in the central, south-western and southern part may likely show saturated and nearly saturated horizons. The north-western, north-eastern and south-eastern parts of the area were prominent with resistivity value ranging between 250 Ωm and 734 Ωm which indicates fractured or fairly weathered basement.

The iso-resistivity contour map at 30 m depth was contoured at 50 Ωm interval as shown in figure 9. The resistivity range of this depth is from 9.56 Ωm to 805.19 Ωm which indicates weathered

and fractured basement rock. The resistivity value of 10 Ωm to 200 Ωm was observed in the central, south-western and southern part may likely show saturated and nearly saturated horizons. The north-western, north-eastern and south-eastern parts of the area are prominent with resistivity value ranging between 250 Ωm and 805 Ωm which indicates fractured or fairly weathered basement.

AQUIFER POTENTIAL

The thickness, layer resistivity and the nature of the weathered layer are important parameters in the groundwater evaluation of the basement complex terrain (Bala and Ike, 2001; Clerk, 1985). The groundwater potential of the study area shows high,

medium and low zones. Eight VES points were delineated as resistivity varying between 108.5 Ω m and 647.1 Ω m with aquifer potential of the area having weathered/fractured thickness range from 11.8 m to 30.7 m (Table 7).

Table 7: Delineated Aquifer Potentials of the Study Area.

S/N	VES Stations	Location Coordinates	Resistivity of Weathered / Fractured Layer (Ω m)	Thickness of Weathered/ Fractured Layer (m)	Depth to Weathered/ Fractured Layer (m)
1	B ₇	N 09 ⁰ 37 ¹ 51.9 ^{II} E 006 ⁰ 35 ¹ 43.7 ^{II}	437.8	17.6	20.6
2	C ₆	N 09 ⁰ 37 ¹ 48.2 ^{II} E 006 ⁰ 35 ¹ 40.3 ^{II}	309.2	23.7	29.3
3	C ₇	N 09 ⁰ 37 ¹ 48.8 ^{II} E 006 ⁰ 35 ¹ 43.2 ^{II}	566.0	17.2	19.9
4	D ₆	N 09 ⁰ 37 ¹ 45.2 ^{II} E 006 ⁰ 35 ¹ 39.7 ^{II}	647.1	30.7	36.0
5	D ₇	N 09 ⁰ 37 ¹ 45.9 ^{II} E 006 ⁰ 35 ¹ 44.4 ^{II}	614.7	12.2	3.2
6	D ₈	N 09 ⁰ 37 ¹ 46.8 ^{II} E 006 ⁰ 35 ¹ 48.5 ^{II}	317.7	11.8	14.8
7	E ₁	N 09 ⁰ 37 ¹ 42.9 ^{II} E 006 ⁰ 35 ¹ 23.2 ^{II}	108.5	14.5	17.8
8	E ₇	N 09 ⁰ 37 ¹ 43.2 ^{II} E 006 ⁰ 35 ¹ 11.8 ^{II}	396.0	11.9	16.1

AQUIFER PROTECTIVE CAPACITY

The longitudinal conductance value ranges from 0.002642 Siemens to 2.340909 Siemens. The longitudinal conductance at VES A₁ is 2.340909 Siemens which has a good protective capacity and VES C₅ is 0.002542 Siemens, poor protective capacity.

50 % of the VES stations has poor aquifer protective capacity with longitudinal conductance value of less than 0.1 Siemens,

while 14.58 % is weakly protected with values between 0.1 and 0.9 Siemens, 22.92 % is moderately protected within the longitudinal conductance range of 0.2 – 0.69 Siemens. 12.5 % is good protected with values between 0.8 – 4.9 Siemens. The contour map in Figure 8 clearly shows high protective capacity in the western and south-western part of the study area and remaining part has very low protective capacity and can be vulnerable to contamination.

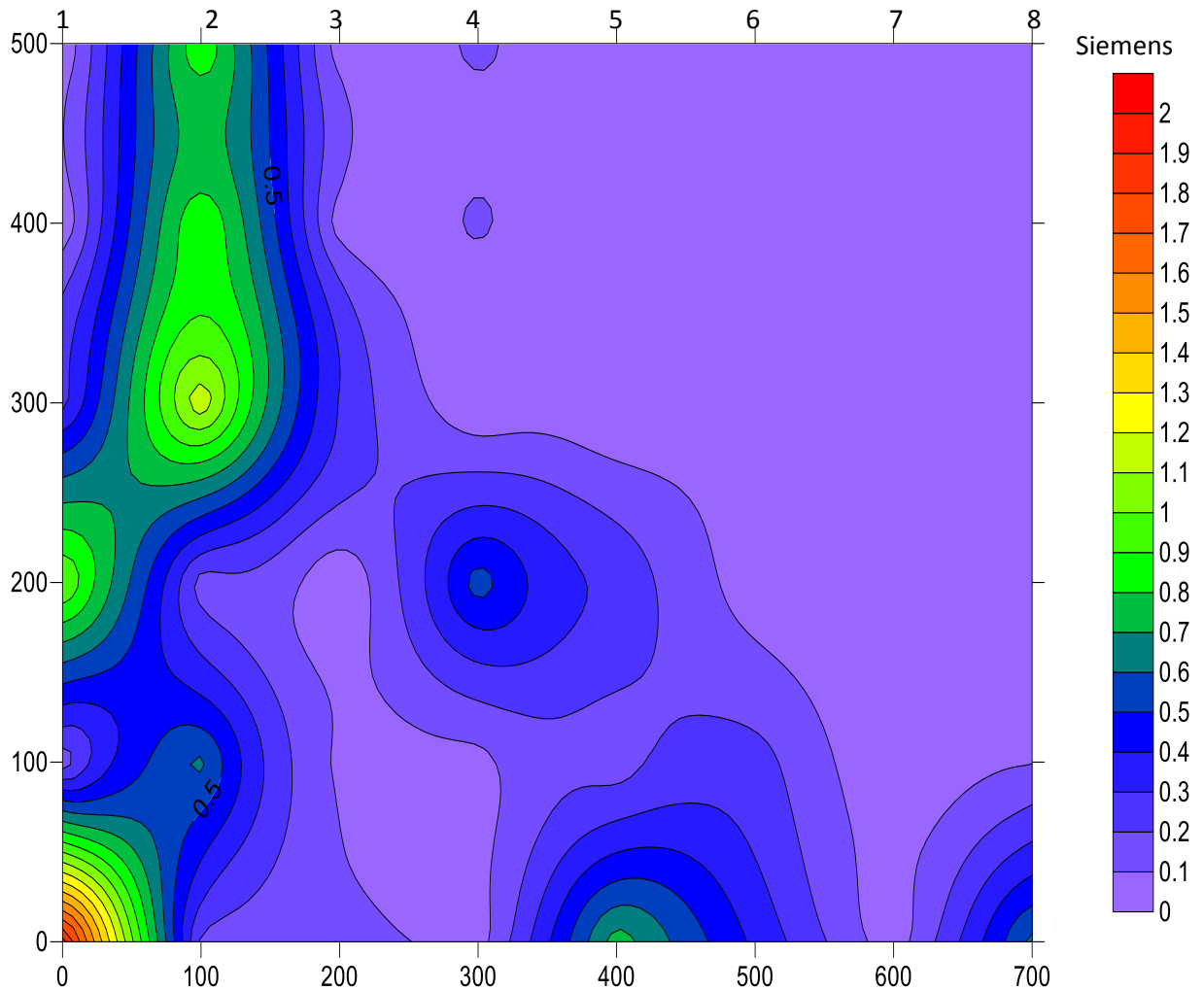


Fig. 8: Contour map of the longitudinal conductance of the area

CONCLUSION

The analysis of the results revealed that the subsurface lithology includes the topsoil, weathered/fractured layer and fresh basement. The weathered layer/fractured layer constitute the major aquifer unit in the area. The curve types were identified as H, HK, K, A and KH. The aquifer's resistivity and thickness values were used to compute the longitudinal conductance of the study area.

The groundwater potential of the study area shows high, medium and low potentials. The study reveals that more than 50 % of the study area has poor aquifer protective capacity with longitudinal conductance value of less than 0.1 Siemens; as, such these area are vulnerable to contamination from infiltration of leachate. The south-western part of the study area shows good protective capacity which can prevents infiltration of leachate.

RECOMMENDATIONS

- Groundwater development should be concentrated around zones that have moderate/very good groundwater potential.
- Areas identified as weak protective capacity should not be drill to avoid contamination.

REFERENCES

- Ajibade, AC (1980): The Geology of the Country around Zungeru, Northwestern state of Nigeria. M.Sc. thesis, University of Ibadan, Ibadan, Nigeria
- Alhassan, DU, Daniel, NO & Okeke, FN (2015). The assessment of aquifer potential and vulnerability of southern Paiko. North Central Nigeria. Using geoelectrical method. *Global journal of Pure and Applied Science* (21). 39-43

- Alhassan DU, Daniel NO and Okeke FN (2017): Geoelectrical Investigation of Groundwater Potentials of Northern Paiko, Niger State, North Central Nigeria. *Journal of Earth Science*, Vol. 28, No 1, pp 103 – 112.
- Bala, AE. & Ike, EC (2001) The Aquifer of the Crystalline Basement Rocks in Gusau Area North-Eastern Nigeria. *Journal of Mining and Geology*. 37, 177 - 184
- Clerk, L (1985). Groundwater Abstraction from Basement Complex Area of Africa. *Journal of engineering Geology London*. 18, 25-34
- Daniel NO, Alhassan DU, Johnson CI, and Okeke FN (2016): Geoelectric Evaluation of Aquifer Potential and Vulnerability of Northern Paiko, Niger State, Nigeria. *Water Environment Research*, Vol.88, No 7, pp 644 – 651
- Kearey, P, Broks, M & Hill, I (2002). An introduction to geophysical exploration. (3rd edition). Oxford U.: Blackwell Science Ltd. Pp 183 – 207.
- Mcginley, M (1969). Aquifer. Retrieved August 26, 2010. <http://eearth.org/article/> Aquifer.
- Telford, WM, Geldart, LP, Sherif, PE. & Keys, DA (1990). Applied Geophysics. Cambridge University Press. Pp. 1-5, 630-640